Introduction

The ability to detect the onset of hemorrhagic shock is of major concern because it remains one of the leading causes of death on the battlefield as well as in civilian trauma cases while also being highly preventable if intervention can be implemented. While mortalities on the battlefield due to shock account for a about 50% of deaths, traumatic injury is the leading cause of death for persons under 45, with 40% mortality before a hospital is reached in civilian settings. With intervention, mortality from hemorrhage drops into the single digit percentages. [1, 2]

In order to detect the onset of hemorrhage accurately and non-invasively trend markers for central blood volume are required. A number of physiological parameters, such as pulse pressure, heart rate variability and baroreflex sensitivity, have been shown to have the potential to provide such early detection. [3] In the case of pulse pressure the physiological connection is quite clear since loss of central blood volume leads to a reduction in stroke volume which in turn reduces arterial pulse pressure. Heart rate variability and baroreflex sensitivity both track changes in autonomic function and frequency domain analysis studies of heart rate variability of intensive care patients have demonstrated that survival was associated with low vagal and high sympathetic tone while the opposite was associated with death. However, because autonomic response is a sensitive marker for many stimuli, it tends to lack specificity.

Recent work suggests that pulse pressure is a sensitive as well as specific marker for central blood loss. [4, 5] If this is indeed the case, the challenge is to develop technologies, both with regard to sensing hardware as well as algorithmic approaches that have sufficient resolution to reliably resolve the comparably small changes in pulse pressure that appear to indicate central blood loss. Detecting progressing hemorrhage therefore amounts to reliably determining changes on the order of a few mmHg in pulse pressures of 35-50 mmHg. Given the separate and unequal uncertainties in determining systole and diastole, such as with brachial cuffs, [6] such determinations are by and large out of reach for today's field-deployable blood pressure measurement technologies until collapse is imminent.

We present here a new approach to tracking blood pressure, and pulse pressure specifically. It is based on a new form of pulse wave analysis, implemented through the Pulse Decomposition Analysis (PDA) algorithm. The PDA algorithm is based on a physical arterial pulse reflection model that analyzes the radial/digital arterial pulse as a superposition of several component pulses, the first of which is the primary left ventricular ejection while the trailing pulses are reflections originating from the central arteries. Referring to **Figure 1** the two major reflection sites to the down-ward traveling arterial pulse are in the region of the renal arteries and in the region beyond the bifurcation of the iliac arteries. The renal reflection site was measured directly by Latham, [7] who performed a detailed experimental study to map out the shape of the pressure pulse in the different sections of the aorta simultaneously using an especially designed catheter with seven spaced micromanometers. At the location of the renal artery the diameter of the aorta, which tapers continuously away from the heart, undergoes its greatest change. This discontinuity presents a significant impedance mismatch to the traveling pressure pulse, as a result of which an appreciable part of its amplitude, about 17%, is reflected. Latham's results also indicated the presence of another reflection site in the vicinity of the bifurcation of the iliac arteries, a region which his micromanometers could not reach.

Other investigators, such as Greenwald, have studied this iliac pulse reflection site. [8] As an aside, an interesting observation made by his group was the fact that this reflection coefficient decreases with age because of changes in abdominal aortic pulse propagation velocity and changes in the bifurcation angle. In recent work, all the central arterial pulse reflections were mapped out by J. Kriz *et. al.* [9], who showed that it is possible to use force plate measurements as a noninvasive

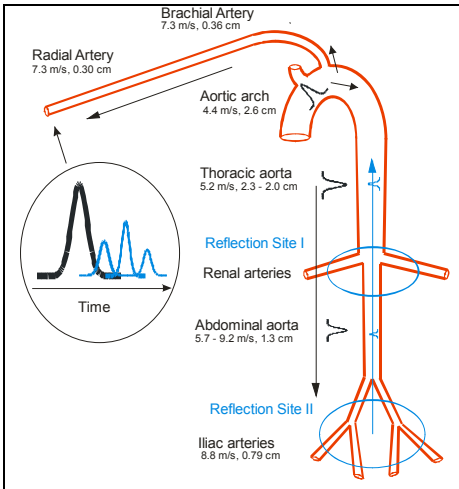

Figure 1: Sketch of the aorta/arm complex arterial system. Two reflection sites, one at the height of the renal arteries, the other one in the vicinity of the iliac bifurcation, give rise to the reflected pulses (blue) that trail the primary left ventricular ejection.

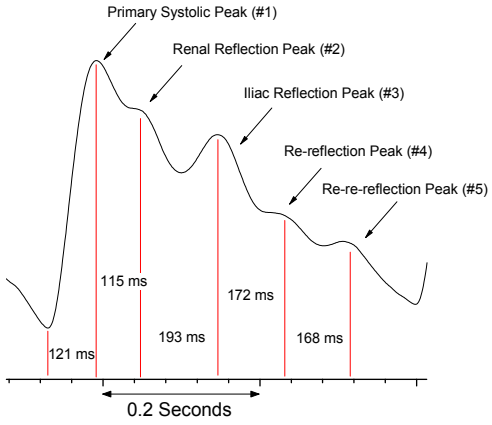

Figure 2: High-fidelity acquisition of a radial pulse line shape. The primary systolic peak is followed by the renal reflection component pulse, then by the iliac reflection, and then by pulses that correspond to re-reflections off the two central artery reflection sites.

method to perform ballistocardiography, which is the motion of the body associated with heart activity and pulse propagation. Interestingly, in addition to the reflected pulses originating from the renal and iliac reflection sites his work also demonstrated the existence of harmonics that arrive even further in time. These pulses are re-reflections of the two reflection sites and, under optimum conditions, it is possible to observe them in pulse line shapes collected at the radial/digital arteries. An example is presented in **Figure 2**.

The PDA algorithm entails isolating, identifying and quantifying the temporal positions and amplitudes of the main three component pulses, that is the primary systolic peak (#1), the renal reflection (#2), and the iliac reflection (#3), within the pulse shape envelope of an individual cardiac cycle. Two pulse parameters are of particular importance. One parameter is the ratio of the amplitude of the renal reflection (#2 pulse) to that of the primary systolic peak (#1). This parameter is referred to as the P2P1 ratio and appears to correlate well with systolic pressure. The second parameter is the time difference in arrival of the primary systolic (#1) pulse and the iliac reflection (#3) pulse. This parameter is referred to as T13 and it appears to correlate with arterial pulse pressure. These preliminary results are based on computer-based modeling of the arterial pulse propagation paths and fitting experimentally obtained temporal component pulse separations and component pulse amplitudes, using arterial wall parameters published in the medical literature, as well as preliminary non-invasive arterial pulse data collections in clinical settings.

The hardware platform that provides the arterial pulse signal for the PDA algorithm's analysis is the CareTaker device. It is a physiological sensing system whose three basic physical components are a sensing pad that couples to the pulsations of the arteries of the middle phalange of the middle digit, a pressure line that pneumatically telemeters the pulsations, and a custom-designed piezo-electric pressure sensor that converts the pressure pulsations into a voltage signal that can be measured, transmitted and recorded. The completely self-contained device wirelessly transmits its signal to a PC computer using the Bluetooth protocol. The device is not occlusive as it operates at a coupling pressure of about 40 mmHg. Another important characteristic of the device is that the signal it provides, sampled at 512 Hz, is the *derivative* of the arterial pulse signal. This provides a significant signal to noise advantage and lowers the resolution requirements for digital acquisition of the signal because the derivative eliminates signal offsets. As a result the signal is always clamped to the signal base line, which in turn allows for increased amplification.

We report here the results of monitoring the evolution of the PDA parameters P2P1 and T13 during the course of lower body negative pressure (LBNP) sessions. LBNP is an established technique used to

physiologically stress the cardiovascular system. It has been used to simulate gravitational stress and hemorrhage, alter preload, and to manipulate baroreceptors. (refs) LBNP was chosen for this project because it has been shown to be very effective at modulating pulse pressure, thereby providing a means to validate the equivalent PDA arterial pulse parameter, T13.

As comparison standards for the bulk of the study we used an automatic brachial cuff as well as a Finapres. We also report the results of a single LBNP session using the Finometer, a modern implementation of continuous blood pressure monitoring based on the Penaz principle.

Patients and Methods

After IRB approval, tests of the CareTaker system were performed at the Cardiovascular Physiology and Rehabiliation Laboratory of the University of British Columbia on fifteen healthy volunteers (average age: 24.4 years, SD: 3.0 years; average height: 168.6 cm, SD: 8.0 cm; average mass: 64.0 kg, SD: 9.1 kg) whose lower bodies, from the height of the navel down, were subjected to increasingly negative pressures. A number of studies have demonstrated that it is possible to simulate significant internal hemorrhage using LBNP. Negative pressures of 10-20 mmHg correspond to 400 to 550 ml of central blood loss, 20-40 mmHg correspond to 500 to 1000 ml, and negative pressures in excess of -40 mmHg correspond to blood losses exceeding 1000 ml. [10]

The subjects were subjected to four stages of negative pressure, -15 mmHg, -30 mmHg, -45 mmHg, and -60 mmHg, each stage lasting typically about 12 minutes. The blood pressure was monitored with an automatic cuff (BP TRU Automated Non-Invasive Blood Pressure Monitor (model BPM-100), VSM MedTech Devices Inc.) set to record blood pressures every three minutes, resulting in typically four readings per LBNP setting as well as an Ohmeda 2300 Finapres, and a pulse oximeter (Ohmeda Biox 3740 Pulse Oximeter, BOC Health Care) monitored oxygen saturation. The CareTaker system collected arterial pulse shapes via a finger cuff attached to the central phalange of the middle digit. Four subjects became presyncopal and could not complete the -60 mmHg LBNP stage.

PDA Algorithm

The basic components of the algorithm are 1. a peak finder that identifies heartbeats in the derivative data stream, 2. the differentiator that produces the second derivative of the detected heart beat which is then used to find the inversions in order to identify the location of the component pulses, 3. an integrator that generates the integrated pulse wave form, from the differentiated raw signal stream, and from which relative component pulse amplitudes are determined and 4. a “hyper-integrator” that allows identification of the primary systolic peak. Furthermore the frequency content of the data stream is continuously analyzed in order to calculate signal to noise (S/N) figures of merit that determine whether signal fidelity is sufficiently high to permit peak detection and analysis.

The peak finder module operates on a rolling buffer array of 40 raw data entries (40 x 12 bit plus 2) that are also low-pass filtered by a single-pole Bessel filter. The detector continuously adjusts its detection thresholds by keeping track of the negative and positive-going variances of the signal relative to the base line. As a result, if the signal fidelity deteriorates the detector’s threshold increases as a percentage of full peak amplitude to keep the number of false triggers low in order to minimize the computational load required for the subsequent pulse analysis.

The frequency content of the pulse stream is continuously assessed to establish whether detection and analysis is feasible. Most of the harmonic content of the heartbeat pulse resides in a frequency band below 30 Hz because the arterial pulse is bandwidth-limited as a result of the low-pass mechanical filtering of the arterial wall. [11] A method that has proven to give a very good figure of merit is taking the ratios of different spectral amplitudes in order to identify the presence of high frequency noise. Frequency band ratios that have shown themselves to be very useful have been the 1-3 Hz and 4-8 Hz

bands as signal bands, whose ratio with a “background” band such as 20-30 Hz can reach values up to 20 for high S/N ratio conditions and deteriorates to decimal fractions for poor S/N conditions.

Once heartbeat peaks are detected, inter-beat intervals and heart rates are calculated. While the inter-beat intervals are tracked and stored individually, the heart rate represents a three inter-beat average. This average is significant because it provides the PDA algorithm an estimate of the dimension of the analysis array that will store a given heart beat spectrum for pulse spectrum analysis. To assure the accuracy of the heart rate calculation, inter-beat intervals are subjected to a series of conditions before they are accepted. Beyond having to be within physiologically plausible boundaries they have to satisfy certain variance conditions, relative to previously detected inter-beat intervals to avoid the inclusion of erroneous outliers.

Once the peak finder has identified and confirmed a peak, a data stream section, whose length is dependent on the heart rate information and that surrounds the detected peak, is loaded into the pulse analysis array. The contents of that array are digitally differentiated, yielding the second derivative of the arterial pulse waveform for purposes of identifying the component pulses, as well as digitally integrated to obtain the arterial pulse.

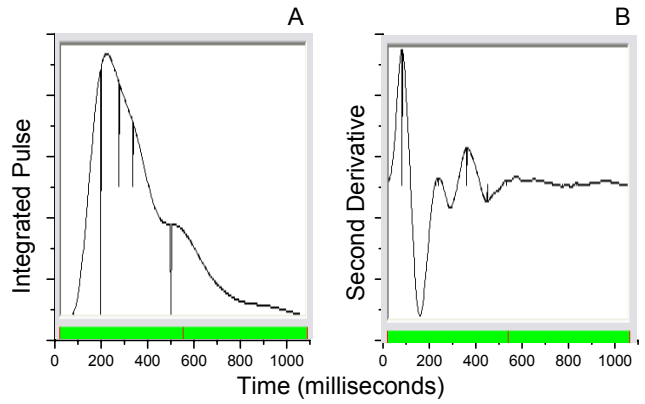

Figure 3: Integrated pulse line shape (A) and 2nd derivative (B), both digitally generated from the CareTaker’s derivative signal stream. Vertical markings at 195 and 490 milliseconds in graph A indicate the presence of the systolic peak and iliac reflection, respectively. Shorter vertical lines mark extend of renal reflection.

The differentiator yields line shapes (**Figure 3B**) that permit another peak detector module to detect the inversions that identify the location of the reflection component pulses while the integrator is implemented in another time domain two-pole low-pass Bessel filter with a roll-off of 20 dB/dec. at 4 Hz. The result of integration is shown in **Figure 3A**.The advantage of using Bessel filters over other time-domain filters is that they are extremely stable.

While the determination of the primary systolic peak in younger or fit subjects is relatively straightforward, since it is the highest peak, it is considerably more challenging in subjects who feature a pronounced “second systolic peak”. In this case the primary peak only amounts to a shoulder, an inversion on the front of the rising heart beat pulse. The most effective detection technique is to integrate the pulse several times, to “hyper integrate”, which amounts to progressively low pass filtering the signal. As a result the fundamental harmonic of the heartbeat spectrum, the systolic peak, is amplified relative to the higher-frequency components, that is, the trailing reflected pulses.

Once the temporal locations of the reflection component pulses and the systolic peak are identified, the T13 interval, which is the time delay between systolic and iliac peak (P3), is calculated. Based on the temporal location of the renal reflection (T2) and the systolic peak permits the determination of the amplitudes of the P2 peak and the systolic peak, in the integrated pulse spectrum, which are then used to calculate the P2P1 ratio.

Statistical Analysis

We present regression coefficients between LBNP levels and systole and pulse pressure responses of the three measurement systems. In order to compare relative sensitivities of the three systems to changes in pulse pressure we present results of different repeated measures ANOVA analyses, which

were performed using the Minitab statistical software (Release 14, Minitab Ltd.). Data are presented as means ± SE unless specified otherwise.

Results

Comparison of Pulse Pressure Changes

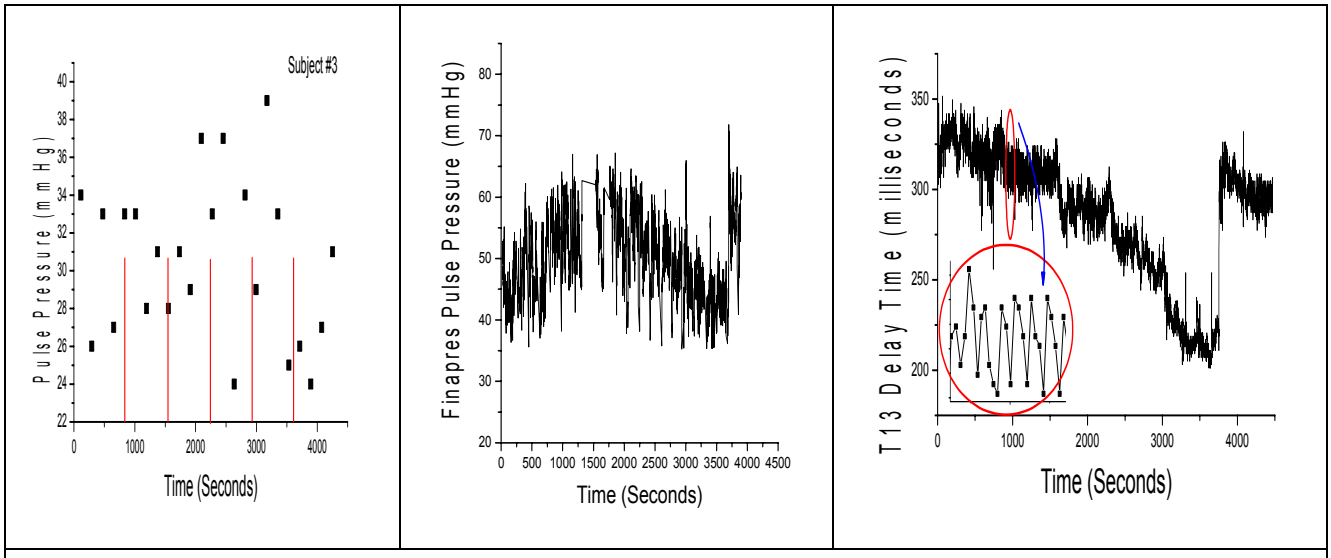

Figure 4: Comparison of the individual results for cuff-based pulse pressure (left graph), Finapres-based pulse pressure (center), and PDA-based T13 measurements, for subject #3. The right panels present the simultaneously obtained T13 delay times between the primary left-ventricular ejection pulse and the iliac reflection pulse recorded on the subject's middle member of the middle digit.

Figure 4 displays a representative side-by-side comparison of pulse pressures obtained with the automatic cuff (left graph) and the Finapres (center graph), as well as the evolution of the T13 parameter over the course of the LBNP session of subject #3, (right graph).

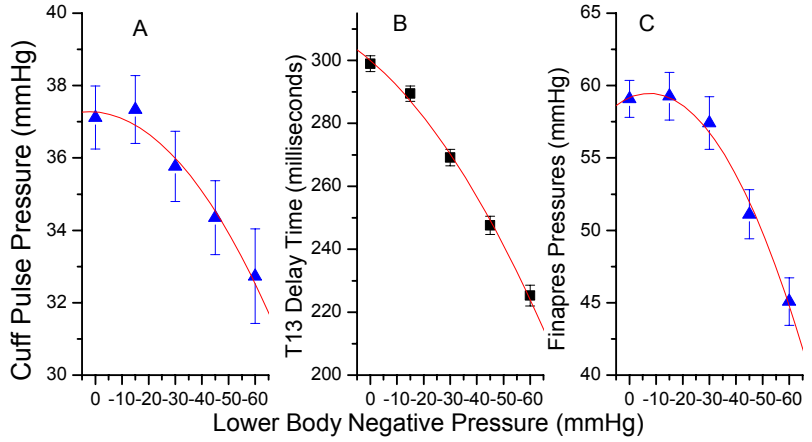

Figure 5: Overall results for pulse pressure obtained with the automatic cuff (graph A), the PDA pulse pressure-equivalent parameter T13 (B) and the Finapres (C).

Figure 5 presents comparative overall results for pulse pressures and T13 as a function of increasing negative pressure. Specifically, **Figure 5A** presents the overall pulse pressure results of the automatic pressure cuff while **Figure 5B** presents the overall results of the pulse pressure-equivalent PDA arterial pulse parameter T13, which is the time difference between the arrival of the primary left ventricular ejection pulse (pulse #1) and the arrival of the iliac reflection (pulse #3). **Figure 5C** presents overall pulse pressure results for the Finapres.

The ability of the three measurement methods to resolve the effects of the different LBNP stages at a statistically significant level varied. While the PDA method was able to resolve each of the four LBNP stages, neither the Finapres nor the cuff were able to resolve the stages with the two lowest negative pressures (-15 & - 30 mmHg) with significance set at $p \leq 0.05$. **Table 1** presents the results of the ANOVA analysis.

Table 1:
ANOVA: PDA, Finapres, Cuff versus LBNP (-15 & -30 mmHg)

```
Factor  Type   Levels  Values
LBNP  fixed       2  1, 2


Analysis of Variance for PDA

Source  DF      SS      MS      F      P
LBNP   1  1113.8  1113.8  48.32  0.0001
Error   92  2120.7    23.1
Total   93  3234.6
S = 4.80119   R-Sq = 34.44%   R-Sq(adj) = 33.72%

Analysis of Variance for Finapres

Source  DF       SS     MS     F      P
LBNP   1     60.3   60.3  0.23  0.636
Error   92  24540.0  266.7
Total   93  24600.3
S = 16.3321   R-Sq = 0.25%   R-Sq(adj) = 0.00%

Analysis of Variance for Cuff

Source  DF       SS     MS     F      P
LBNP   1    403.8  403.8  1.57  0.214
Error   92  23688.4  257.5
Total   93  24092.2
S = 16.0463   R-Sq = 1.68%   R-Sq(adj) = 0.61%
```

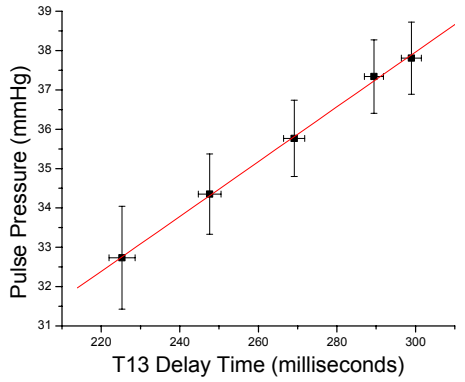

Figure 6: Correlation between T13 PDA parameter and pulse pressure.

Of interest also is the degree to which the PDA parameter T13 correlates with arterial pulse pressure. Based on the results presented in **Figure 5** the T13 parameter and the pulse pressures determined with the cuff and the Finapres appear to have a non-linear dependence on central blood loss. If they are indeed equivalent, they should be linearly related to each other. **Figure 6**, which correlates averaged values for both devices, suggests a linear correlation. Also, the correlation provides a conversion factor for relating T13 values to pulse pressures for individuals with T13 values in the neighborhood of 300 milliseconds (0.19 x T13 (milliseconds) + 2.58).

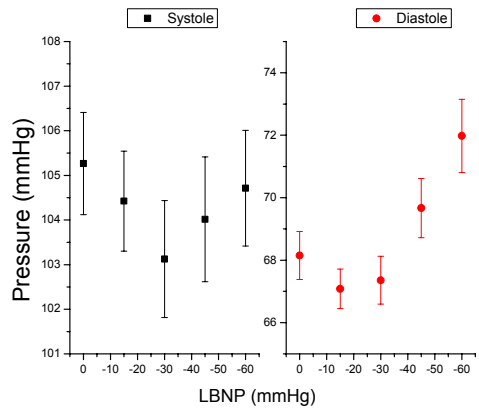

Figure 7: Overall study results for systolic and diastolic blood pressures obtained with the automatic cuff.

Comparison of Systolic & Diastolic Blood Pressure Changes

In regard to the systolic blood pressure recorded with the automatic cuff, next to no correlation with LBNP was determined. The diastolic pressure showed a modest increase with increasing LBNP. These results, for the cuff only, are presented in **Figure 7**. They are in contrast to those reported in the Convertino reference,[12] which reported a decline in systolic pressure of 18 mmHg with increasing LBNP (same range as used here) and next to no change in diastolic pressure in a cohort of subjects with an average age of 15 years older than the subjects studied here.

In contrast to the cuff results and in support of the results of the Convertino study, the PDA parameter that is equivalent to systolic pressure, the P2P1 ratio, did show a statistically significant decrease with LBNP. This decrease was also observed in the data obtained with the Finapres continuous blood pressure monitor. These results, which are presented in **Figure 8**, further support the conclusions reached by others that neither systole nor diastole have been shown to be generally applicable and reliable indicators for central hypovolemia.

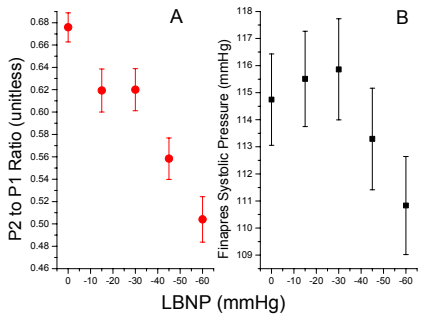

Figure 8: Overall results for the P2P1 ratio (A), the PDA parameter that is equivalent to systolic pressure, and the Finapres systolic pressure (B), as a function of LBNP.

Of particular interest, in regard to correlating changes in PDA parameters with those in blood pressure, is the rebound in systole that was observed in all 15 subjects when the negative pressure in the chamber was released. **Figure 9** presents a correlation of the PDA parameter P2P1 versus systole obtained with the Finapres, collected at -60 mmHg and 0 mmHg. Each point represents a 15-second average of individual heart beats. The correlation is 48.77 x P2P1 + 98.33.

In regard to the discrepancy between the automatic cuff results obtained in the Convertino study and in this study it is important to note that the blood pressure ranges reported here are very small, on the order of 5 and 8 mmHg in the case of the systolic and diastolic pressures, respectively. It is very difficult to resolve blood pressure trends within such small limits with automatic brachial cuffs due to their instrumental uncertainties and differences in proprietary algorithms. As an example, one study that compared the performance of brachial cuffs and catheters revealed standard deviations (SD) on the order of 12 mmHg with essentially zero bias in the case of systolic blood pressures and SDs of the order of 12 mmHg as well as a positive bias of 10 mmHg in the case of diastolic pressure measurements. [13]

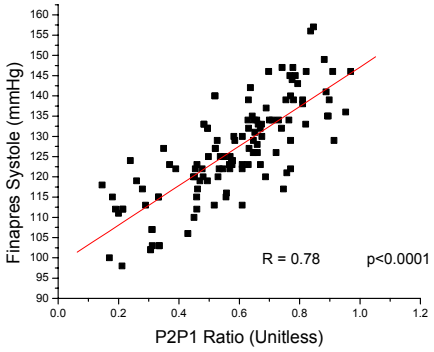

Figure 9: Correlation of P2P1 ratio with Finapres systole for -60 mmHg and 0 mmHg LBNP.

Comparison with Finometer

A separate test of the CareTaker system was performed at the US Army Institute of Surgical Research at Fort Sam Houston. In this experiment a 59 year old male underwent the same LBNP procedure described above, except that the negative pressure stage times were shortened to five minutes. The gold standard in this case was a Finometer (Finapres Medical Systems, Amsterdam, The Netherlands), which is a FDA-approved modern version of the Finapres. **Figure 10** displays side-by-side comparisons of the pulse pressure determined using the Finometer and the T13 parameter obtained with the CareTaker/PDA system. The inspiratory effort-related modulations are displayed in a detailed blow-up of the data.

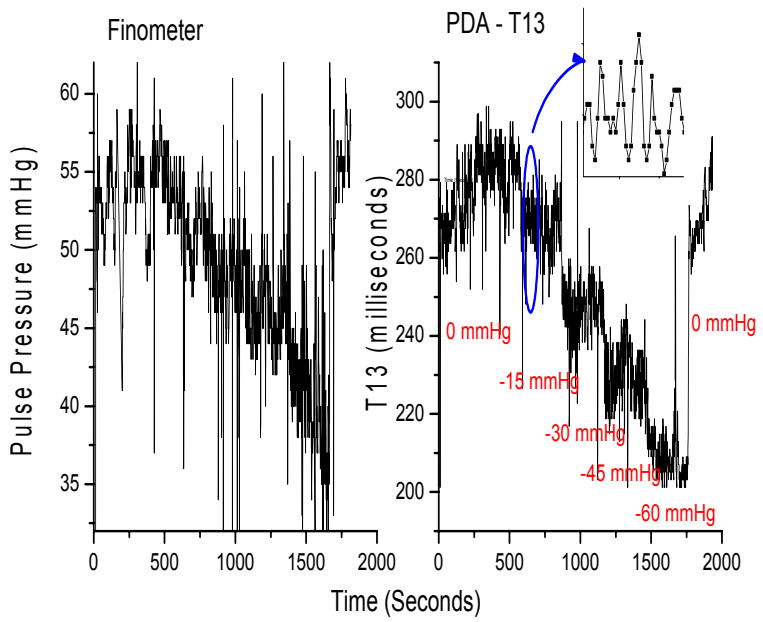

Figure 10: Temporal evolution of the arterial pulse pressure, measured with a Finometer (left graph), and the T13 parameter determined by the CareTaker system over the course of an LBNP run with a 58 y. old male. Wide band signal in T13 trace is not noise but due to respiratory sinus arrhythmia-induced pulse pressure modulations.

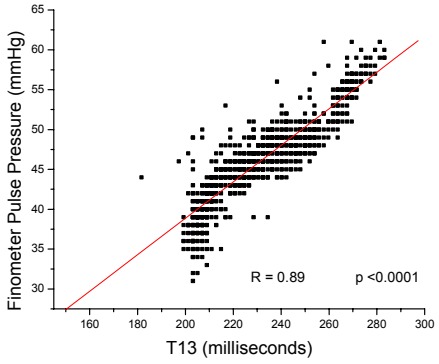

Figure 11: Beat-by-beat correlation of T13 with Finometer pulse pressure.

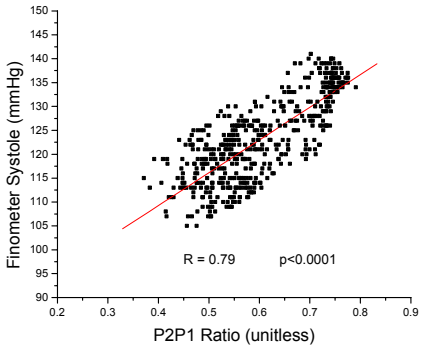

Figure 12: Beat-by-beat correlation of P2P1 with Finometer systolic pressure.

Figures 11 & 12 give the linear correlations of, respectively, T13 with the Finometer pulse pressure (0.22896 x T13 (in milliseconds) -6.92) and P2P1 with the Finometer systolic pressure (68.6 x P2P1+81.79).

Discussion

The PDA model

The statements regarding P2P1 and T13 are based on a pulse propagation model of the delay times with which the individual pulses will arrive at the radial/digital artery. In the set of equations below, t_n refers to the arrival time of the nth pulse. X1 refers to the arm arterial path while x2, x3 refer to the thoracic and abdominal aorta, respectively. The primary pulse, #1, will traverse a part of the aortic arch, which is ignored as it is part to all the path lengths, and will then traverse the arteries of the arm x1 traveling at a pulse velocity that is in the pressure regime of systole. In the set of equations the equation relating pressure and velocity (Moens-Korteweg) is provided in the

$$t_1 = \frac{x_1}{v_{arm,systole-R1*PP}}, \qquad where \qquad v = \sqrt{\frac{hE_0 e^{\xi P}}{2\rho\alpha}}$$

$$t_2 = \frac{x_2}{v_{aorta1,systole}} + \frac{x_2}{v_{aorta1,diastole+R2*PP}} + \frac{x_1}{v_{arm,diastole+R2*(1-R1)*PP}}$$

$$t_3 = \frac{x_3}{v_{aorta2,systole-R2*PP}} + \frac{x_2}{v_{aorta1,systole}} + \frac{x_3}{v_{aorta2,diastole+R3*(1-R2)*PP}} + \frac{x_2}{v_{aorta1,diastole+R3*(1-R2)*(1-R2)*PP}} + \frac{x_1}{v_{arm,diastole+R3*(1-R2)*(1-R2)*(1-R1)PP}}$$

$$t_4 = \frac{x_3}{v_{aorta2,systole-R2*PP}} + \ldots$$

upper right corner. The definitions are as follows: $v_{x,P}$ is the velocity of the xth arterial pulse path at the pressure P indicated. E is the Young's modulus, α is the artery's diameter, h is the arterial wall thickness, ρ is the fluid density, ξ is the arterial compliance and P0 is the pressure and PP is the pulse pressure. The Young's modulus and the arterial extensibility ξ are of course different for different arteries. The terms describing the path length of the "second systolic" pulse are as follows. It traverses the thoracic aorta at systolic pressure, traverses is again as an R2 reflection after re-direction at the renal arteries (indicated as R2 of pulse pressure plus diastolic pressure) and then enters the arm arteries where is loses another percentage of its amplitude due to the R1 reflection coefficient that incorporates artery segment transitions, such as the aortic/subclavian junction. R1 is actually irrelevant because all component pulses are equally affected by it.

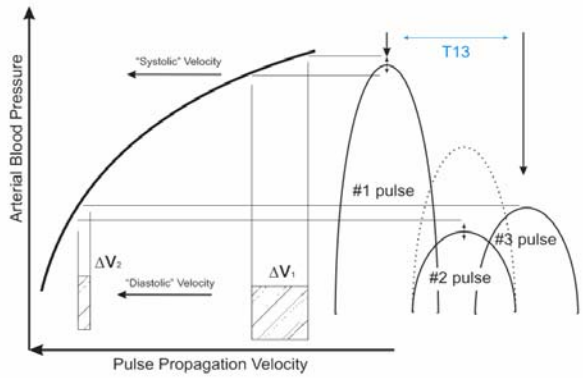

Figure 13: Relative amplitudes and velocity/pressure relationships of the component pulses. P2's amplitude and propagation velocity can change significantly due to the pressure dependence of R2, the renal reflection coefficient.

Another critical feature of the model is that R2, the renal reflection coefficient, is dependent on systolic pressure. The motivation for this is based on the following consideration. The renal reflection originates at the junction between thoracic and abdominal aorta, a junction that is characterized by a significant change in arterial diameter. It was already pointed out by Latham [7] that this junction can be readily modulated by increasing the pressure within the thorax and thereby reducing the transmural pressure, such as during a valsalva maneuver. In this case the thoracic aorta's diameter shrinks relative to the diameter of the abdominal aorta and the impedance mismatch of the junction is reduced. One then observes a significant drop in the amplitude of the renal reflection at the radial or digital arteries. Conversely, if the pressure within the thoracic aorta rises, increasing transmural pressure, the artery will expand. Since the thoracic aorta is the softest artery in the body, and in particular much more extensible than the abdominal aorta, increasing peak pressure, or systole, will enlarge the diameter mismatch, giving rise to a more pronounced renal reflection pulse amplitude. The critical insight then is that the amplitude of the renal reflection will increase relative to the amplitude of the primary systolic (#1) peak because, while both component pulses travel the arteries of the arm complex, and are therefore both subject to the pulse narrowing and heightening due to the taper and wall composition changes of the peripheral arteries, only the renal reflection will have sampled the pressure-induced aortic impedance mismatch changes. This establishes the motivation for taking the ratio of the amplitudes of the #2 and the #1 pulse, that is P2P1.

A similarly plausible argument can be made for the difference in arrival times of the primary pulse (#1) and the iliac reflection (#3), or T13. The difference in the arrival times of the primary arterial pulse, that is the left ventricular ejection, and the iliac reflection pulse is determined by the differential velocities with which both pulses propagated along their arterial paths. In the case of the iliac reflection the path length is longer than that of the primary pulse by almost twice the length of the torso. More importantly, the pulse's arterial propagation velocities are pressure dependent, a relationship long known through the Moens-Korteweg equation.[18] One central insight is that both pulses travel at different velocities because their pressure amplitudes are different, the iliac reflection pulse amplitude, which is determined by the reflection coefficient of the iliac reflection site, being on the order of 40% of pulse pressure. This point is graphically made in **Figure 13**. Both pulses therefore load the arterial wall differently during their arterial travel, as a result of which their propagation velocities are different. The second insight is that, because the pressure/velocity response curve is non-linear, a result known since the 1960s based on Anliker's work,[19] both pulses accelerate and decelerate at different rates as the pressure rises and falls. The primary pulse experiences the highest changes in velocity as a function of

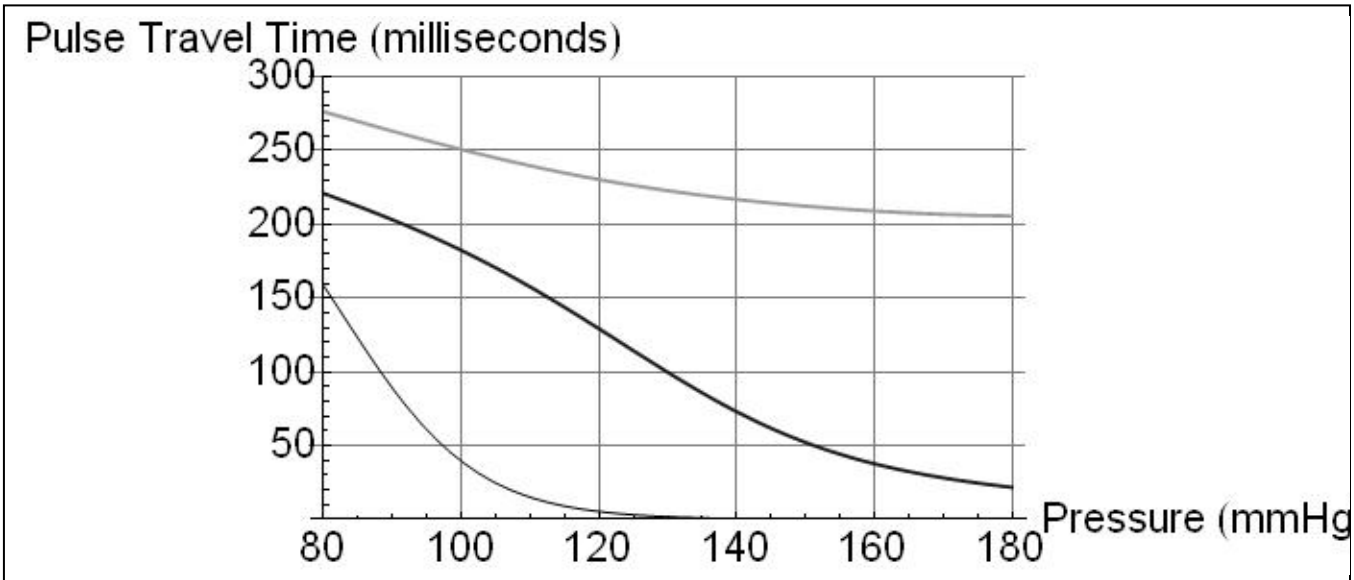

Figure 14: Arrival times, as predicted by PDA model, of the three component pulses, from bottom up, P1, P2 (renal reflection), and P3 (iliac reflection).

changes in blood pressure because it is subject to the steepest section of the pressure/velocity response curve, while the iliac pulse, "running" at much lower pressure, changes velocity much more gradually. Changes in the time of arrival therefore then reflect changes in the differential arterial pressure that the two pulses experience. While this differential pressure is not exactly pulse pressure, that is the difference between the full pulse arterial pulse height and the diastolic pressure floor, it represents about 60%-70% of it, assuming the previously stated iliac reflection coefficient.

Figure 13 presents a graphic display of the relative amplitudes of the left ventricular ejection (P1) and the trailing reflection pulses and their resulting relative positions on the pulse propagation velocity curve, which is highly pressure dependent. As a result the arrival times of the different pulses are highly pressure dependent, a point that is clarified by **Figure 14**, which presents the pulse travel times, from top to bottom, respectively, of the iliac, the second systolic, and the primary ejection pulse. The iliac pulse's arrival shortens only slightly with increasing pressure because its amplitude remains close to the diastolic pressure regime. The second systolic peak's arrival time (middle) experiences significant non-linearity because the reflection coefficient, R2, is highly pressure dependent, as a result of which is can cross into the "systolic" pressure regime. The left ventricular ejection (P1, bottom curve) has the highest amplitude and samples the steepest section of the pressure/velocity curve and is therefore most pressure dependent. Using Young's moduli obtained from the literature and letting the model fit R2 as well as the velocities of the primary arterial path ways it is then possible to compare experimental data with model predictions.

Succinctly put, **Figure 14** displays the fact that the human body is very short relative to arterial pulse propagation velocities. Human arterial pathways, for the average height population we have studied, are generally very short relative the distances the arterial pulse traverses within a cardiac cycle at typical arterial pulse propagation velocities that range, for healthy and unstressed arteries, from 4 – 9 m/s. This fact influences particularly the arrival time of the P1 pulse profoundly. In the lower pressure range, which is the pressure regime that was examined here, the P1 pulse pulls away from the P2 and P3 reflection pulses, as evidenced by the fact that its arrival time shortens significantly faster with increasing pressure than the arrival times of P2 and P3. Consequently, in this pressure range, T13 would be expected to widen with increasing pressure and shorten with decreasing pressure. **Figure 14** therefore provides a quantitative basis for why T13 would be directly dependent on blood pressure changes in the blood pressure regime that was examined here.

As the pressure continues to increase, however, the arrival time of the primary pulse saturates as it runs out of arterial runway. Consequently further increases in arterial pulse propagation velocity do not result in a further shortening of the arrival time. Meanwhile P3 continues to accelerate with increasing pressure, narrowing the T13 time delay in this high-pressure regime. The details of the pressure-dependent evolution of the arrival time curves are critically dependent on the choice of different velocity profiles for the different arterial sections, a point that is discussed in the following section.

Comparison with model predictions

Using the experimental T13 and blood pressure values it is now possible to compare these with the predictions of the PDA model and to explore the relative temporal behavior of the component pulses.

In **Figure 15** we present an overlay of the experimental results and the model's predictions. The experimental data, all averages from 15 subjects, are the T13 values obtained from each LBNP stage as well as the corresponding pulse pressure values as determined with the Finapres. Since systole did not change appreciably for any of the subjects, we use the average value of 120 mmHg throughout. The most important aspect of the agreement between the model and data, as presented in **Figure 15**, are the arterial parameter assumptions that are required to achieve it. The single dominant factor that determines the response of T13 to pressure changes is the pressure/arterial pulse velocity response of the different arterial sections that the systolic pulse and its two central reflections traverse. It further turns out that the range of relative pressure/velocity response curves that is possible, given the constraints of the experimental data, is very narrow. **Figure 16** presents the relative response curves of the three arterial segments that constitute the pulse pathways, the thoracic aorta, the abdominal aorta, and the arm complex arteries. Clearly the model at this stage uses a significant simplification of the arterial path sections and the response curves presented represent averages over these pathways. While more details will be introduced in future versions of the model the aim here is to demonstrate that the basic physical picture hypothesized by the PDA model matches observations.

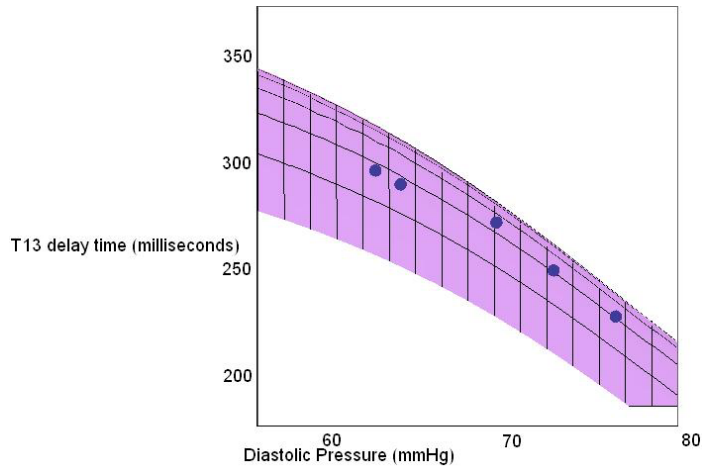

Figure 15: Overlap of PDA T13 prediction and LBNP study data as a function of diastolic pressure change. The line around which the data are grouped corresponds to systole = 120 mmHg. Adjacent lines correspond to ±5 mmHg.

While the starting values for the pressure/velocity curves presented in **Figure 16** are based on published arterial pulse propagation velocities, [14] the results of the LBNP experiments provide an opportunity to deduce the relative dynamic response characteristics of the different sections, which are not readily available as they have not been the subject of research interests in a long time. The distinguishing feature of the pressure velocity curves presented in **Figure 16** is the dramatically different dynamic behavior of the arm complex relative to that of the central arteries. Specifically, while the arm complex arteries display a distinct exponential response characteristic, the central arteries display, in the blood pressure range under consideration, an essentially linear response. And it is this difference in dynamic response that enables the model to generate T13 curves whose slopes match those observed. In contrast, changes in starting values amount only to offsets that shift the family of curves in parallel up or down in but do not change the relative slopes of the curves.

A significant benefit of measuring T13 over pulse pressure directly could be its higher resolution and sensitivity. The results indicate the equivalence of a change of about 200 milliseconds in T13 to a variation of about 8 mmHg in pulse pressure *over the entire range* of a simulated central blood loss in excess of 1 liter for this cohort of fit and relatively young subjects. The results therefore indicate that the PDA technology is capable of resolving small changes in pulse pressure, a feat that particularly automated cuffs are not well suited for. Given the suggestion by others that pulse pressure can be considered as a surrogate for stroke volume and therefore as a means to track loss of blood volume in trauma patients(4), the accurate monitoring of pulse pressure could be a vital component in predicting the onset of hemorrhage.

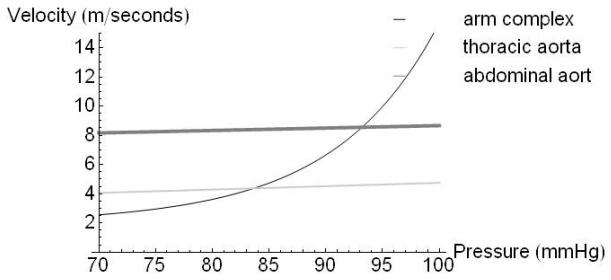

Figure 16: Arterial pulse velocity profiles based on fit to experimental results in Figure 15.

Conclusions

We have presented a new physical model of the propagation of the arterial pressure pulse and its reflections as well as compared the predictions of the model with experimentally obtained pulse parameters and conventionally obtained blood pressures. The agreement of observations and measurements provides a preliminary validation of the model which in turn could provide a renewed impetus in the study of the human arterial pressure pulse. The model is based on few, and very physical, assumptions, because it proposes that the structure of the pulse is due to it is readily identifiably arterial pulse reflection sites. As a result it is also readily testable. One example is aortic aneurysms. Both results by Kriz and using the CareTaker / PDA technology, which will be reported elsewhere, have demonstrated that the central arterial pulse reflections are modified by the presence of aortic aneurysms because the additional reflection sites interfere with the renal and iliac reflection sites.

It is hoped and the likelihood is high that this study will yield new insights into vascular health and central pressure issues that transcend the launch of a product that has very significant market potential by any measure. If the PDA model is fully validated it could have a significant impact on today's medical view of arterial pulse reflections and their health implications.

[1] Bellamy RF. The causes of death in conventional land warfare: implications for combat casualty care research. *Mil Med.* 1984;149:55–62.

[2] Carrico CJ, Holcomb JB, Chaudry IH, PULSE trauma work group. Post resuscitative and initial utility of life saving efforts. Scientific priorities and strategic planning for resuscitation research and life saving therapy following traumatic injury: report of the PULSE trauma work group. *Acad Emerg Med.* 2002;9:621– 626.

[3] Cooke WH, Salinas J, Convertino VA, et al. Heart rate variability and its association with mortality in pre-hospital trauma patients. *J Trauma.* 2006;60:363–70; discussion 370.

[4] Convertino VA, Cooke WH, Holcomb JB, Arterial pulse pressure and its association with reduced stroke volume during progressive central hypovolemia, J Trauma. 2006 Sep;61(3):629-34.

[5] Leonetti P, Audat F, Girard A, Laude D, Lefrere F, Elghozi JL.Stroke volume monitored by modeling flow from finger arterial pressure waves mirrors blood volume withdrawn by phlebotomy.*Clin Auton Res.* 2004;14:176 –181.

[6] Davis, JI, Band MM, et. al, Peripheral blood pressure measurement is as good as applanation tonometry at predicting ascending aortic blood pressure, J. of Hyperten. 2003, 21:571–576.

[7] Latham, RD *et. a*l, Regional wave travel and reflections along the human aorta: a study with six simultaneous micromanometric pressures. *Circulation* **72**, 1985, 1257-69.

[8] Greenwald SE, Carter AC and Berry CL, Effect of age on the in vitro reflection coefficient of the aortoiliac bifurcation in humans, Circulation, Vol 82, 114-123, 1990

[9] Kriz J. et al, Force plate measurement of human hemodynamics, *Nonlinear Biomed Phys.* 2008 Feb 22;2(1):1

[10] Cooke, William H, and Convertino, Victor A, Heart Rate Variability and Spontaneous Baroreflex Sequences: Implications for Autonomic Monitoring During Hemorrhage, J. Trauma, Injury, Infection, and Critical Care, 58(4):798-805, April 2005.

[11] Callaghan FJ et. al, The relationship between arterial pulse-wave velocity and pulse frequency at different pressures, Med Biol Eng Comput. 1986 May;24(3):248-54.

[12] Convertino VA, Cooke WH, Holcomb JB, Arterial pulse pressure and its association with reduced stroke volume during progressive central hypovolemia, J Trauma. 2006 Sep;61(3):629-34.

[13] Davies JI, Band MM, Pringle S, Ogston S, Peripheral blood pressure measurement is as good as applanation tonometry at predicting ascending aortic blood pressure, J. of Hypertension. 21(3):571-576, March 2003.

[14] MacDonald's, *Blood Flow in Arteries,*4th ed. Arnold,1998.